ESL-TR-94/12-08

November 1994. To be published in the 1995 ASME Int'l Solar Energy Conference Proceedings.

A Modified Analytical Method for Simulating Cyclic Operation of Vertical U-Tube Ground-Coupled Heat Pumps

Monte K. Dobson
Exxon Production Research Company
Houston, Texas

Dennis L. O'Neal
Department of Mechanical Engineering
Texas A&M University
College Station, Texas

William Aldred
Department of Agricultural Engineering
Texas A&M University
College Station, Texas

ABSTRACT

A modified analytical model is presented which discretizes the ground-coupled heat exchanger of a ground-coupled heat pump and utilized a separate cylindrical source solution for each element. First law expressions are utilized for each element to derive a set of fully implicit finite difference equations for the pipe wall temperature and the fluid temperature profile inside the ground-coupled heat exchanger. This method entails less computational overhead than methods which utilize numerical solutions inside the soil, and comes closer than previous analytical methods to satisfying the constant heat flux assumption of the original analytical solution. The thermal capacitance effects of the fluid inside the ground-coupled heat exchanger are included to allow proper prediction of the entering water temperature (EWT) profile at start-up. Comparisons with experimental data on EWT, capacity, energy input and cycling are provided.

DEFINITION OF SYMBOLS

c	Liquid Specific Heat (kJ/kg-K)
COP	Coefficient of Performance (dimensionless)
EWT	Water Temperature Entering Water-Refrigerant Heat Exchanger (^oC)
G	Cylindrical Integral (dimensionless)
h	Convection Coefficient (W/m^2-K)
k	Thermal Conductivity (W/m-K)
m	Mass (kg)
$\dot{m}$	Mass Flow Rate (kg/s)
Nu	Nusselt Number (dimensionless)
p	Dimensionless Radius (dimensionless)
Q'	Heat Transfer Rate/Unit Length (W/m)
R	Thermal Resistance (K/W)
R'	Thermal Resistance/Unit Length (K-m/W)
r	Radius (m)
Re	Reynolds Number (dimensionless)
T	Temperature (^oC)
t	Time (min or sec)
z	Fourier Number (dimensionless)
u	Velocity (m/s)

DEFINITION OF GREEK SYMBOLS

a	Thermal diffusivity (m^2/s)
b	Integrative variable
DT	Temperature Difference (^oK)
g	Dimensionless variable
h	Dimensionless variable
l	Dimensionless variable
c	Dimensionless variable
m	Kinematic Viscosity (m^2/s)
r	Density (kg/m^3)

DEFINITION OF SUBSCRIPTS

c	Capacity or Cycle
cond	Condenser
d	Diameter
f	Fluid (Water)
ff	Far-Field
g	Ground to Pipe Interface
gc	Ground-Coil
i	Inner
l	Load
o	On or Outer
s	Soil
w	Inner Pipe Wall

INTRODUCTION

Over the past 20 years, there has been renewed interest in utilizing the ground as a heat source/sink for heat pumps. Using the soil rather than the ambient air as the heat source in

heating and the heat sink in cooling offers potential thermodynamic advantages since the earth is normally at a more favorable temperature for heat extraction or rejection. Quantifying the performance of ground-coupled heat pumps (GCHPs) requires an accurate assessment of the water temperature entering the GCHP (EWT). An accurate model must account for the heat transfer interactions between the GCHP, the circulating fluid, and the soil. The modeling process is complicated by various factors such as thermal interaction between adjacent tubes and the transient nature of the heat transfer which occurs due to on/off cycling of the GCHP.

Models of ground-coupled heat exchangers have proceeded in two different directions: (1) numerical solutions of the heat diffusion equation in the soil and the ground-coil [Mei and Fischer, 1984] and (2) modified analytical solutions [Al-Juwayhel, 1981; Bose et al., 1985; Deerman, 1991]. The numerical solutions, while based on fewer assumptions than the analytical solutions, require significant run times. They were intended primarily as a check of simpler models or for performing parametric analyses [Cane and Forgas, 1991].

Two analytical solutions have been employed previously to model ground-coupled heat exchangers, the Kelvin line source solution [Ingersoll et al., 1954; Claesson and Dunard, 1983], and a cylindrical source solution [Jaeger, 1940, 1942; Carslaw and Jaeger,1959]. Both predict the temperature field as a function of radius and time in an infinite medium of constant properties bounded internally by a constant heat flux source. The line source solution assumes the source is of zero radius, and is therefore inaccurate for simulating finite diameter pipes for values of dimensionless time (at/R^2) less than 20 [Ingersoll et al., 1954]. For the system simulated in this study, this requirement corresponded to a heat pump on-time of 78 minutes. The average heat pump on-time was only 21 minutes, though, and significant transients were exhibited in the first minute of the on-cycle [Dobson, 1991]. The necessity of an accurate solution for short times rendered the line source solution inappropriate for the present study.

The model presented herein utilizes the cylindrical source solution to simulate a ground-coupled heat pump, with the cyclic behavior of the GCHP determined by a load model of the building structure. This method includes several important improvements over previous methods. First, the ground-coil is discretized into elements for which the assumption of spatially uniform heat flux is more appropriate. Second, thermal interaction between adjacent legs of the heat exchanger is modeled directly by superposition, rather than utilizing steady-state solutions modified by empirically determined constants [Deerman, 1991]. Third and most importantly, the model simulates the GCHP on a time scale that is small enough to capture the transient phenomena within individual cycles and over longer time intervals. Neither moisture migration within the soil nor soil freezing around the ground-coil are modeled, hence the model is not appropriate where either of these phenomena is expected to be important.

The purpose of this paper is to present, in detail, the mathematical model which is summarized above. This mathematical model was implemented into a computer program which has been successfully verified against experimental data [Dobson, 1991].

MODEL DEVELOPMENT

The constant heat flux solution for a finite diameter pipe (or cylindrical source solution), as presented by Ingersoll et al. [1954], is as follows:

$$T_g(r,t) - T_{ff} = \frac{Q' G(z,p)}{k_s} \qquad (1)$$

where: Q' = heat flux per unit length
$z = at/r_o^2$,
$p = r/r_o$, and

$$G(z,p) = \frac{1}{\pi^2}\int_0^\infty \frac{\left(e^{-\beta^2 z} - 1\right)}{J_1^2(\beta) + Y_1^2(\beta)}\left[J_0(p\beta)Y_1(\beta)J_1(\beta)Y_0(p\beta)\right]\frac{d\beta}{\beta^2}$$

The integral expression for G was solved numerically at various z for integer values of p from 1 to 10 for this study.

The heat flux and the far-field temperature of the soil (T_{ff}) vary with both distance along the ground-coil and with time. The coil is divided into elements for which the assumption of spatially uniform heat flux is more acceptable. A separate solution is then applied for each element. To allow for temporal variations in heat flux for each element, the method of superposition, originally suggested by Ingersoll [1954], is used. In this way, the temperature rise from the far-field to the pipe wall (T_g-T_{ff}, or DT_g) is represented as the sum of the temperature rises caused by the heat inputs for each prior time increment. The value of time used in the

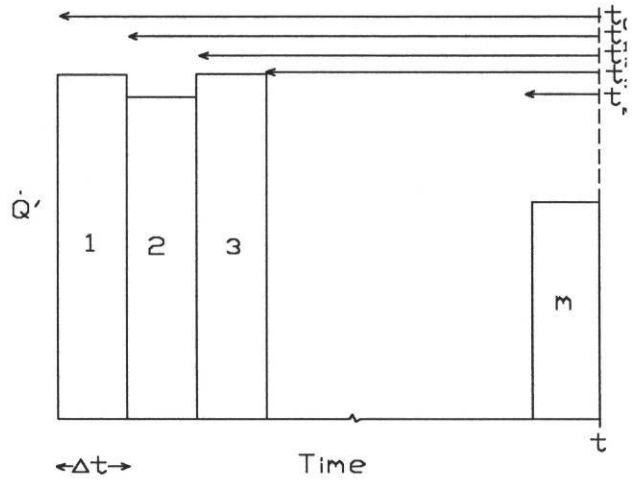

FIGURE 1 -METHOD OF SUPERPOSITION FOR CYLINDRICAL SOURCE SOLUTION

Fourier number (z) for each increment is the time since the particular interval began or ended, not the time since calculations began (Figure 1). The methodology is equivalent to imposing a positive heat input at the beginning of the time interval in conjunction with a negative heat input of the same strength at the end of the time interval [Claesson and Dunard, 1983]. When applying this methodology to a series of m heat inputs, one obtains:

$$\Delta T_g = \frac{1}{k_s}\left[\sum_{j=1}^{m-1} Q'_i * \left[G(z(t_{j-1}),p) - G(z(t_j),p)\right]\right] + \frac{Q'_m * G(z(t_{m-1}),p)}{k_s} \qquad (2)$$

With a method in place for computing the soil temperature at the pipe wall, the task remains of formulating the finite difference equations for solving the fluid temperature field inside the pipe. Figure 2 presents a schematic of the computational domain, and the unknown temperatures. Because the fluid temperatures are defined at the ends of the elements rather than in the middle, it is necessary to define a mean fluid temperature for each element:

$$\overline{T}_{fi} = \frac{T_{fi} + T_{fi+1}}{2} \tag{3}$$

Also, the major assumptions made for each element include:

1. Thermal interference from adjacent legs of the U-tube is modeled using superposition,
2. Heat conduction is one dimensional in (r) the soil,
3. The thermal storage capacity of the pipe wall is negligible,
4. Axial conduction inside the fluid is negligible,
5. Radial temperature gradients inside the fluid are negligible, and
6. The convection coefficient and all thermal properties are constant.

Modeling the thermal interference by superposition partitions the temperature rise at each leg of the U-tube into a contribution from itself and its thermal interference partner. The temperature rise from the thermal interference partner represents an average around the circumference of the tube, since the temperature rise around the circumference varies. This approach is clearly an approximation, but more realistic than treating the U-tube as an equivalent single tube since varying U-tube separations can be modeled.

On cycle

Using the aforementioned assumptions, an energy balance on each fluid element yields:

$$\dot{m}c\left(T_{fi} - T_{fi+1}\right) - hP\Delta z\left(\overline{T}_{fi} - T_{wi}\right) = \rho A_c \Delta z c \frac{\overline{T}_{fi}^{p+1} - \overline{T}_{fi}^{p}}{\Delta t} \tag{4}$$

Equation 4 states that the net energy entering the element by advection minus the energy leaving the element by convection equals the time rate of change of internal energy within the element. The fully implicit finite difference method was utilized in the present study, so that all temperatures on the left hand side of Equation 4 should be evaluated at time p+1. This method is unconditionally stable.

Equation 4 can be rearranged by separating terms in p and p+1:

$$T_{fi}^{p+1}\left(1-2\eta+\lambda\right) + T_{fi+1}^{p+1}\left(1+2\eta+\lambda\right) - 2\lambda T_{wi}^{p+1} = T_{fi}^{p} + T_{fi+1}^{p} \tag{5}$$

where,

$$\eta = \frac{\dot{m}\Delta t}{\rho A_c \Delta z} = \frac{u\Delta t}{\Delta z}$$

$$\lambda = \frac{2h\Delta t}{\rho c R}$$

In the present study, it is assumed that no thermal resistance exists between the pipe and the earth. If an appropriate value were known, however, it could be combined in series with the thermal resistance of the U-tube.

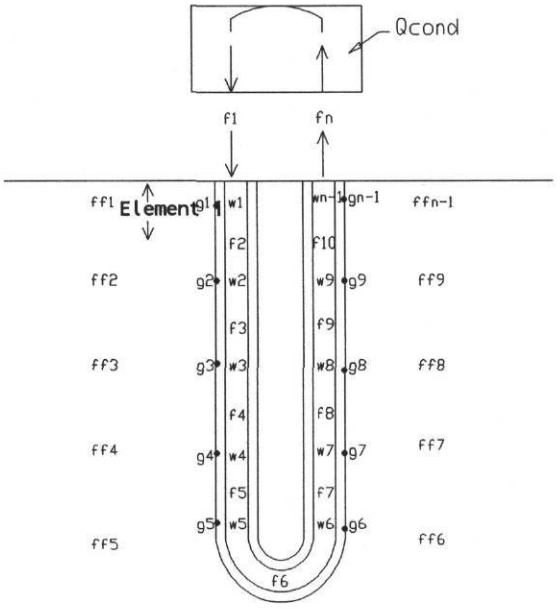

FIGURE 2 - SCHEMATIC OF COMPUTATIONAL DOMAIN AND UNKNOWN TEMPERATURES

The convection coefficient (h) in the above equations was calculated using the Dittus-Boelter correlation [Incropera and Dewitt, 1985] which is acceptable for $Re_d > 10{,}000$ and Prandtl numbers between 0.7 and 160. These conditions were both met for all regions of the ground-coil in this study.

If n denotes the number of fluid temperatures and n-1 denotes the number of elements (or wall temperatures), Equation 5 generates n-1 equations and 2n-1 unknowns. One additional equation is obtained by writing an energy balance on the condenser:

$$\dot{m}c\left(T_{fn} - T_{f1}\right) + \dot{Q}_{cond} = mc\frac{\overline{T}_{fn}^{p+1} - \overline{T}_{fn}^{p}}{\Delta t} \tag{6}$$

Evaluating the left hand side at time p+1, representing Q_{cond} as a linear function of T_{fn} $\left(a_o + a_1 T_{fn}\right)$, and defining h as above, one obtains:

$$T_{f1}^{p+1}\left(1+2\eta\right) + T_{fn}^{p+1}\left(1-2\eta-\frac{2a_1\Delta t}{mc}\right) = \frac{2a_0\Delta t}{mc} + T_{f1}^{p} + T_{fn}^{p} \tag{7}$$

In addition to Equation 7, n-1 additional equations are obtained by employing Equation 2 to calculate T:

$$T_{gi}^{p+1} = T_{ffi}^{p} + \frac{1}{k_s}\left[\sum_{j=1}^{m-1} Q'_j * G\left(z(t_{j-1}),1\right) - G\left(z(t_j),1\right)\right] + \frac{Q'_m G\left(z(t_{m-1}),1\right)}{k_s} \quad (8)$$

In Equation 8, j is used to subscript the prior heat inputs for element i, with the m^{th} being the final heat input. The j^{th} heat input for the i^{th} element can be written as:

$$Q'_j = hP * \left(\overline{T}_{fi}^{p+1} - T_{wi}^{p+1}\right). \quad (9)$$

Equation 9 is used to compute Q'_j for each time increment once the temperatures are known for time p+1. Thus, all terms in the summation of Equation 8 are known. The quantity Q'_m, however, contains unknown fluid and inner wall temperatures at time p+1. Equation 8 also adds a new set of unknowns, the outer wall temperatures T_g. Because the thermal capacitance of the pipe is neglected, the convective heat flux at any time is equal to the conductive heat flux through the pipe:

$$hP\left(\overline{T}_{fi} - T_{wi}\right) = \frac{T_{wi} - T_{gi}}{R'} \quad (10)$$

where: $$R' = \frac{\ln\left(\frac{r_o}{r_i}\right)}{2\pi k_{pipe}}$$

Imposing Equation 10 at time p+1, solving for T_{gi}^{p+1}, substituting this into Equation 8, and grouping terms in p+1 yields:

$$T_{wi}^{p+1}(1+2\gamma) + T_{fi}^{p+1}(-\gamma) = T_{ffi}^{p} + \frac{1}{k_s}\sum_{j=1}^{m-1} Q'_j * \left[G\left(z_{j-1},1\right) - G\left(z_j,1\right)\right] \quad (11)$$

where: $$\gamma = \frac{G(z_{m-1},1)hP}{2k_s} + \frac{hPR'}{2}.$$

In Equation 11, all G values are understood to be for a p value of 1. The subscripts on the z values refer to the time values to be used. Equation 11 adds n-1 equations to the n equations previously written, thereby closing the problem mathematically (assuming that initial conditions are known).

Recalling that the U-tube configuration has two pipes dissipating heat near one another, it is apparent that Equation 11 must be altered to include the effect of the other leg of the U-tube. This is often referred to as thermal short circuiting, and is modeled using superposition [Claesson and Dunard, 1983]. With this method, DT_g includes the effect of both legs of the U-tube.

Applying the method of superposition to compute the surface temperature of element i, whose "thermal interference partner" is element k, at the end of the m^{th} heat input, one obtains:
The G values for element i utilize a p value of 1 because the temperature is desired at the pipe wall of element i. For element j, the G values are computed for a p value which is the ratio of the distance between the two pipe centers to the radius of pipe i (Figure 3). When computed in this way, the outer pipe wall

$$T_{wi}^{p+1}(1+2g) + T_{fi}^{p+1}(-g) + T_{fi+1}^{p+1}(-g) + T_{wk}^{p+1}(2f) + T_{fk}^{p+1}(-f) + T_{fk+1}^{p+1}(-f) = T_{ffi}^{p} \frac{1}{k_s}\sum_{j=1}^{m-1} Q'_{ij} * \left[G(z_{j-1},1) - G(z_j,1)\right] + Q'_{kj} * \left[G(z_{j-1},p) - G(z_j,p)\right] \quad (12)$$

where: $$f = \frac{G(z_{m-1},p)hP}{2k_s}$$

temperature is an average value over the pipe surface because there are angular temperature variations around the pipe.

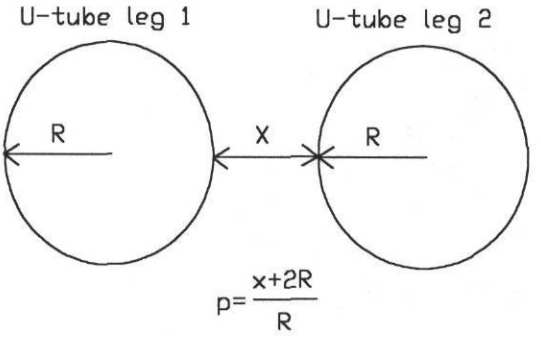

Figure 3 - Geometric Definition of p for Two Neighboring Elements

It should be noted that for the two elements at the bottom of the U-tube, two fluid temperatures which are subscripted differently in Equation 12 actually refer to the same fluid temperature (the one at the bottom). The correct coefficient for this fluid temperature is the sum of both coefficients which reference it.

Provided that the same time step and indoor air conditions are used throughout the simulation, all coefficients of the p+1 terms are time invariant. Thus, the coefficient matrix can be inverted before simulation begins and multiplied at each time step by the new row vector provided by the right hand side of Equations 5, 7, and 12. This is considerably faster than solving a new set of equations at each time step.

Off cycle

Equations 5, 7, and 12 are derived assuming that the unit and the water circulating pump are on. A GCHP cycles on and off to meet the cooling load on the home, however, so this condition is not met at all times. These equations must be re-evaluated during the off cycle. For Equation 5, the advection term vanishes and the convective heat transfer changes from forced convection to free convection. The necessary changes can be accomplished merely by setting h equal to zero, and remembering that h must be computed with a free convection coefficient. Kavanaugh [1984] determined a bulk free convection coefficient for an entire U-tube with water as the fluid, and obtained a value of 137 W/m^2-K which was used in this study.

The true physical model for the condenser element during the off cycle is much more complicated. First, the advection term vanishes as the water circulating pump shuts off. Second, the heat supplied to the water, which during the on cycle represents the capacity and power input of the refrigeration cycle, changes as the refrigeration cycle is halted. These are both of the energy exchange modes accounted for in Equation 7, and when they

vanish it merely degenerates to state that the fluid temperatures do not change with time. During the off cycle, the water actually exchanges heat with both the refrigerant in the condenser and the ambient air. The only mode of energy transport accounted for in the present model is free convection with the ambient air. Thermal storage capability of the condenser wall is again neglected, so the heat transfer from the water in the condenser to the ambient air can be framed in resistance concepts. The energy balance then yields:

$$\frac{T_{amb} - \overline{T}_{fn}^{p+1}}{R_t} = mc\frac{\overline{T}_{fn}^{p+1} - \overline{T}_{fn}^{p}}{\Delta t} \tag{13}$$

where: $R_t = R_{conv,i} + R_{cond} + R_{conv,o}$

$$R_{conv,i} = \frac{1}{2\,\pi\, r_i\, \Delta z\, h_i}$$

$$R_{cond} = \frac{\ln\frac{r_o}{r_i}}{2\,\pi\,\Delta z\, k_{pipe}}$$

$$R_{conv,o} = \frac{1}{2\,\pi\, r_o\, \Delta z\, h_o}$$

Grouping Equation 13 into terms for time p and time p+1, one obtains:

$$T_{fn}^{p+1}(1+c) + T_{f1}^{p+1}(1+c) = T_{fn}^{p} + T_{f1}^{p} + 2cT_{amb} \tag{14}$$

where: $c = \dfrac{\Delta t}{m\, c\, R_t}$

Unlike Equations 5 and 7, Equation 14 remains valid during the off cycle. The only necessary modification is that the convection coefficient inside the tube be changed from a forced convection coefficient to a free convection coefficient.

Initial Conditions

The analytical solution to the soil temperature distribution of Equation 1 assumes that the temperatures are initially uniform in the radial direction for each element. This would be acceptable if one always started simulations at the time the heat pump began operation. This is not always desirable or feasible, however. The effect of the initial conditions can be included by characterizing the heat rejection history of the ground-coil. The prior heat inputs contribute to the temperature increase DT_g in the same way as "old" heat inputs do during a simulation, and are appended to the prior heat inputs at each time step. The value of time to be used in the Fourier number is again the time since the heat input began, not the time since the beginning of simulation. The temperature increase at the pipe wall (p=1) caused by n heat inputs which served as initial conditions and m heat inputs which occurred since the simulation began is:

$$\Delta T_g = \frac{1}{k_s}\left[\sum_{i=1}^{n} Q_i * (G(z(t_{i-1}),1) - G(z(t_i),1)) + \sum_{j=1}^{m} Q_j * (G(z(t_{j-1}),1) - G(z(t_j),1))\right] \tag{15}$$

The m^{th} heat input in Equation 15 is included in the summation (unlike Equation 2), but the result is the same because the value of G for t_m is equal to zero.

LOAD AND CYCLING MODEL

To model the cyclic behavior of the heat pump, two first law relations are used. First, assuming that the thermostat is not changed, an energy balance over a complete cycle yields:

$$\int_0^{t_c} \dot{Q}_l\, dt - \int_0^{t_{on}} \dot{Q}_c\, dt = 0 \tag{16}$$

Next, an energy balance over the on-time only yields:

$$\int_0^{t_c} \dot{Q}_l\, dt - \int_0^{t_{on}} \dot{Q}_c\, dt = 0 = (mc)_{home}\,(T_2 - T_1) \tag{17}$$

The right hand side of Equation 17 represents the amount of energy removed from the home during the on-time. For the site simulated, this quantity and a simplified load model of the residence were estimated from experimental data [Dobson, 1991].

When a cycle began, the energy input via the load and the energy extracted via the capacity were set to zero. For each time step, the energy added (load) and the energy removed (capacity) were calculated and added to the respective totals. The unit was kept on until the energy removed minus the energy added was greater than $-(mc)_{home}\,(T_2 - T_1)$. After the unit cycled off, no energy was removed for the remainder of the cycle. Thus, at each time step the energy added was incremented until it equaled or exceeded the energy removed for the cycle. When this condition was met, a new cycle began and the process was repeated.

MODEL VERIFICATION

The model was verified with actual data from a field-monitored, 10.5 kW GCHP which is located in Abilene, TX. Details of the unit and experimental measurements on the unit are available in a previous paper (Dobson et al., 1992). Predictions were compared to field data from September 3 to September 7, 1990, a five day period during which data were continuously collected on time intervals of 5 minutes or shorter. The actual load was computed from experimental data and used as input to verify the ground-coil model independently of errors in load prediction. Monitored data were also used to deduce the ground-coil heat rejection history which was needed for initial conditions. The fraction of the total heat which was dissipated in each element was computed from results of a seven day simulation with no initial conditions.

The simulation began on September 1 to allow the program to accumulate several days of actual heat inputs in common with the unit before comparisons were begun. The load was computed using weather data from the National Weather Service in conjunction with a field-determined regression equation until the first data on short time intervals were available (9:00 A.M. on September 3). Actual load data were available from this date

until September 7 at 10:30 A.M. The load for the rest of September 7 was computed using a field-determined load model [Dobson, 1991].

Knowledge of the thermal conductivity, k, and the thermal diffusivity, a, is required for simulation purposes. This is normally the limiting factor in the accuracy of GCHP simulations [Kavanaugh, 1984]. Deerman [1991] suggested using a model based on the constant heat flux cylindrical source solution to determine k and a. He used a 6-hour continuous cycle and adjusted both properties to obtain a good fit of the data. At the Abilene installation, however, the density was known from soil core samples which were taken at depths up to 30.5 m. The results of this core sample are presented in Table 2. An average value of density weighted by depth was estimated as 2080 kg/m^3. Also, data from Deerman [1990] showed that the specific heat for a large variety of soils was approximately 0.84 kJ/kg-^oK. Knowledge of these properties meant that only the thermal conductivity, k, had to be estimated from field data. Estimated average values of k and a were 1.73 W/m-^oK and 9.72×10^{-7} m^2/sec, respectively.

The daily experimental EWT for September 3 through September 7 were compared to the simulation results. Figure 4 shows a comparison of the smoothed curve fits of the means of the experimental and simulated data for September 4. This figure shows that the model tracks the daily trends in EWT quite well, being accurate to within 0.8 ^oC most of the time. The model also showed similar agreement between the simulated and experimental EWT for the other days between September 3 and 7. Verifying the model against actual usage patterns presents a more challenging and more useful test than the long, continuous cycles often chosen for verification.

TABLE 2 - RESULTS OF SOIL CORE SAMPLES

Depth (m)	Density (kg/m^3)	Moisture Content %	Porosity	Description
.8-1.4	1631	10.3	.382	Sandy Clay: Reddish-Brown
2.3-2.6	1988	3.6	.261	Silty Sand: Reddish-Brown, with gravel
4.7-5.1	1871	15.2	.327	Weathered Shale: Reddish-Brown
7.2-7.6	1887	14.1	.318	Weathered Shale: Reddish-Brown
10.8-11.0	2167	9.5	.217	Weathered Shale: Reddish-Brown
11.7-12.2	2138	11.3	.225	Weathered Shale: Reddish-Brown
14.9-15.2	1911	12.8	.310	Shale: Reddish-Brown
18.0-18.3	2057	13.8	.257	Shale: Reddish-Brown
22.6-22.9	2025	12.6	.274	Shale: Reddish-Brown
27.4-27.6	2250	7.7	.188	Shale: Reddish-Brown
30.2-30.5	2274	7.6	.175	Shale: Reddish-Brown

The data in Figure 4 are useful for verifying that the model is representative of the data over long time periods, but offers little insight as to how it tracks start-up data. A more detailed view is provided in Figures 5, which presents the simulated and experimental values of EWT over a 22 minute on-time which began at approximately 11 A.M. on September 4. Both the model and the experimental data showed the rapid decrease in EWT at start-up as the water from the bottom of the ground-coil entered the condenser. The prediction of the minimum EWT by the model following the off cycle never differed from the measured value by more than 1.1 ^oC. One limitation of the model appears to be that it is stiffer than the actual physical system in that it under predicts the cooling of the water during the off cycle. One possible reason for this discrepancy is that constant soil properties were used for all elements in the simulation, while the core samples show that the soil properties actually varied significantly with depth. The higher density at greater depths normally corresponds with an increased conductivity, which would allow greater cooling of the water at the bottom of the coil during the off cycle. The value used in the simulation represents an average over the entire coil which appears to work well for normal cycling patterns. The stair-step effect of the simulated data occurred because EWT was output to one decimal place only.

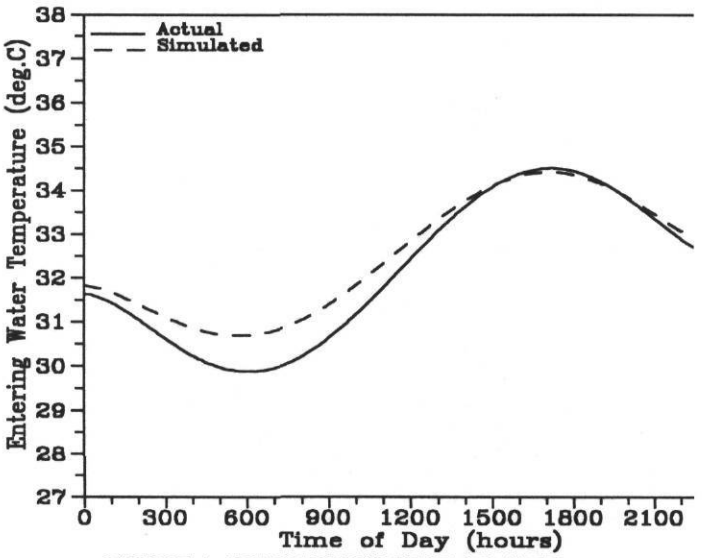

FIGURE 4 -COMPARISON OF SIMULATED AND EXPERIMENTAL EWT VALUES ON SEPTEMBER 4, 1990

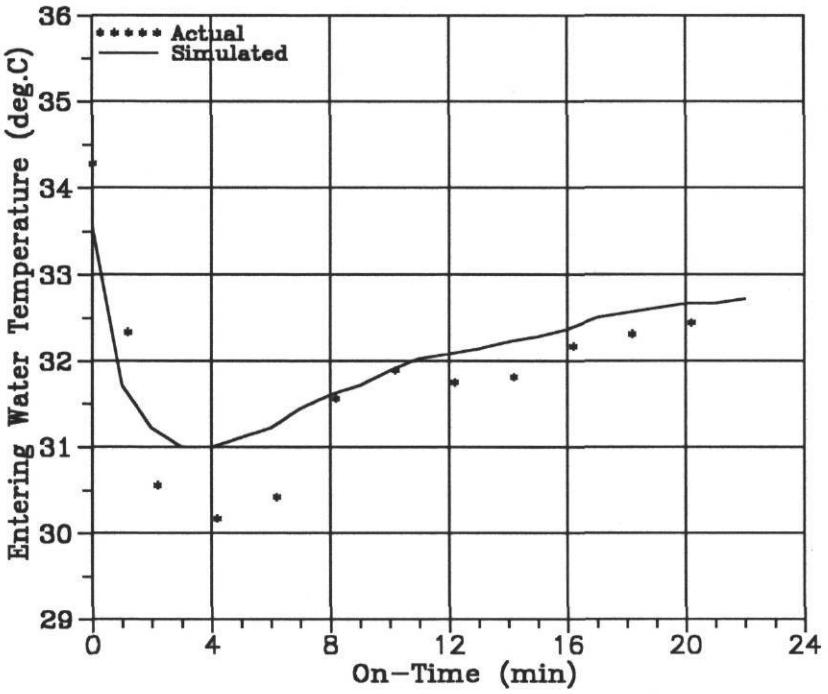

FIGURE 5 - COMPARISON OF SIMULATED AND EXPERIMANTAL EWT VALUES DURING A 22-MINUTE ON-TIME

Daily comparisons of the energy input, heat removal from the home, coefficient of performance (COP), EWT, and number of cycles are presented in Table 3. The data verify that the model accurately simulates the physical system. The most important quantity is the daily COP, which had a maximum percent error of less than 5% and an average percent error of slightly over 2%. The cyclic behavior was also well simulated, as indicated by the nearly identical numbers of cycles per day. The largest error was on September 7, and occurred during the period from 10:30 A.M. until 4:10 P.M. when actual load data were not available for input to the model. The load was slightly under predicted, which allowed the simulated unit to cycle more frequently than the actual system. The daily averaged EWT values were within 0.9 ^{o}C in the worst case, and within 0.3 ^{o}C on the average

TABLE 3 - DAILY COMPARISONS BETWEEN MODEL PREDICTIONS AND EXPERIMENTAL DATA FROM SEPTEMBER 3 TO SEPTEMBER 7.

Date	Q_{out} (kWh)		E_{in} (kWh)		COP (Wh/Wh)		EWT (^{o}C)		# of Cycles	
	Exp.	Model	Exp.	Model	Exp.	Model	Exp.	Model	Exp.	Model
9/3*	69	69	21.5	22.1	3.19	3.12	33.2	32.7	20	21
9/4	94	100	29.9	32.4	3.14	3.09	33.1	33.1	27	28
9/5	113	114	36.6	37.7	3.07	3.03	33.9	33.9	24	23
9/6	105	108	33.6	35.9	3.12	2.97	33.4	34.3	14	13
9/7*	93	88	31.0	29.4	2.99	2.99	34.8	34.5	14	19

* Data on September 3 are from 9:00 A.M. until midnight.
Data on September 7 are from midnight until 4:10 P.M.

SUMMARY

A numerical model is presented which utilizes the analytical solution of a constant heat flux cylindrical source emitting into an infinite medium to predict the soil temperature at the pipe wall of a vertical U-tube GCHP. The coil is discretized into elements for which the assumption of spatially uniform heat flux is acceptable, and a separate analytical solution is used for each element. The fluid temperatures inside the coil are solved for using a fully implicit finite difference scheme. Thermal interference between adjacent legs of the U-tube is accounted for by using superposition.

A computer program was written to solve the mathematical model. This model was verified against field-data for a 5-day period in September for which data on short time-intervals were available. The model tracked experimental data well, with an average difference between predicted daily average EWT and the

experimentally determined value of only 0.3 ^{o}C. The model also successfully simulated the rapid decrease in EWT at start-up, although the model appeared to not allow the water to cool as much during the off cycle as did the physical system. This discrepancy is believed to have been caused by the use of constant soil thermal properties throughout the coil, when in actuality the thermal properties varied with depth.

ACKNOWLEDGEMENTS

This work was supported by the Texas Energy Research in Applications Program.

REFERENCES

Al-Juwayhel, F. I., "Simulation of the Dynamic Performance of Air-Source, Earth-Source, and Solar Assisted Earth-Source Heat Pump Systems", Ph.D. Dissertation, Oklahoma State University, 1981.

Bose, J. E., Parker, J. D., and McQuiston, F. C., Design/Data Manual for Closed-Loop Ground-Coupled Heat Pump Systems, ASHRAE, 1985.

Cane, R. L. D. and Fugas, D. A., "Modeling of Ground Source Heat Pump Performance," ASHRAE Transactions, pp. 909-917, Vol. 97, Pt. 1, 1991.

Carslaw, H. S., and Jaeger, J. C., Conduction of Heat in Solids, Clarendon Press, Oxford, 1959.

Claesson, J., and Dunard, A., "Heat Extraction from the Ground by Horizontal Pipes - A Mathematical Analysis", Swedish Council for Building Research, Document D1, 1983.

Deerman, J. D., "Simulation of Vertical U-Tube Ground-Coupled Heat Pump Systems Using the Cylindrical Heat Source Solution", ASHRAE Transactions, Vol. 97, Pt. 1, 1991.

Dobson, M. K., "An Experimental and Analytical Study of the Transient Behavior of Vertical U-Tube Ground-Coupled Heat Pumps in the Cooling Mode," M.S. Thesis, Texas A&M University, May 1991.

Dobson, M. K., O'Neal, D. L., and Wolfe, M. L., "A Non-Dimensional Analysis of Vertical Configuration Ground-Coupled Heat Pump Start-up", Solar Engineering 1992, ASME/JSEE/KSES International Solar Energy Conference, pp. 367-379, April 5-8, 1992, Maui, Hawaii.

Incropera, F. P., and DeWitt, D. P., Fundamentals of Heat and Mass Transfer, John Wiley & Sons, 1985, New York.

Ingersoll, L. R., and Plass, H. J., "Theory of the Ground Pipe Heat Source for the Heat Pump," Transactions ASHRAE, pp. 339-348, Vol. 54, 1948.

Ingersoll, L. R., Zobel, O. J., and Ingersoll, A. C., Heat Conduction with Engineering, Geological, and Other Applications, McGraw-Hill, 1954, New York.

Jaeger, J. C., "Radial Heat Flow in Circular Cylinders with a General Boundary Condition", Journal of the Royal Society of New South Wales, V. 74, pp. 342-352, 1940.

Jaeger, J. C., "Heat Flow in the Region bounded Internally by a Circular Cylinder", Proceedings of the Royal Society of Edinburgh, V. 61, pp. 223-228., 1942.

Kavanaugh, S. P., "Simulation and Experimental Verification of Vertical Ground-Coupled Heat Pump Systems", Ph.D. Dissertation, Oklahoma State University, 1984.

Mei, V. C, and Fischer, S. K., "A Theoretical and Experimental Analysis of Vertical, Concentric-Tube Ground-Coupled Heat Exchangers," Oak Ridge National Laboratory Contract-153, 1984.